

Supporting information for

**Dimensionality Control in Crystalline Zinc(II) and Silver(I) Complexes with
Ditopic Benzothiadiazole-Dipyridine Ligands**

Teodora Mocanu^{1,2}, Nataliya Plyuta³, Thomas Cauchy³, Marius Andruh^{1,*} and Narcis Avarvari^{3,*}

¹ Inorganic Chemistry Laboratory, Faculty of Chemistry, University of Bucharest, Str. Dumbrava Rosie nr. 23, 020464, Bucharest, Romania; teo_mocanu_sl@yahoo.com

² Coordination and Supramolecular Chemistry Laboratory, “Ilie Murgulescu” Institute of Physical Chemistry, Romanian Academy, Splaiul Independentei 202, Bucharest 060021, Romania

³ MOLTECH-Anjou, UMR 6200, CNRS, UNIV Angers, 2 bd Lavoisier, 49045 Angers Cedex, France ;
plyutanataliya@gmail.com (N.P.); thomas.cauchy@univ-angers.fr (T.C.)

* Correspondence: marius.andruh@dnt.ro; narcis.avarvari@univ-angers.fr

IR spectra

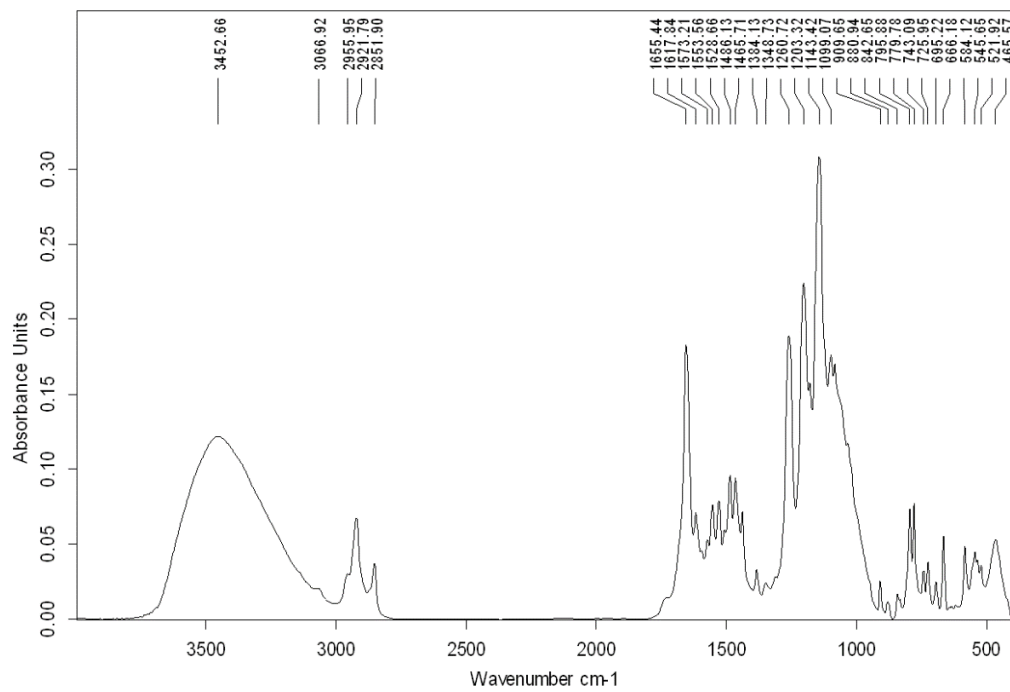


Figure S1. IR spectrum of compound 1.

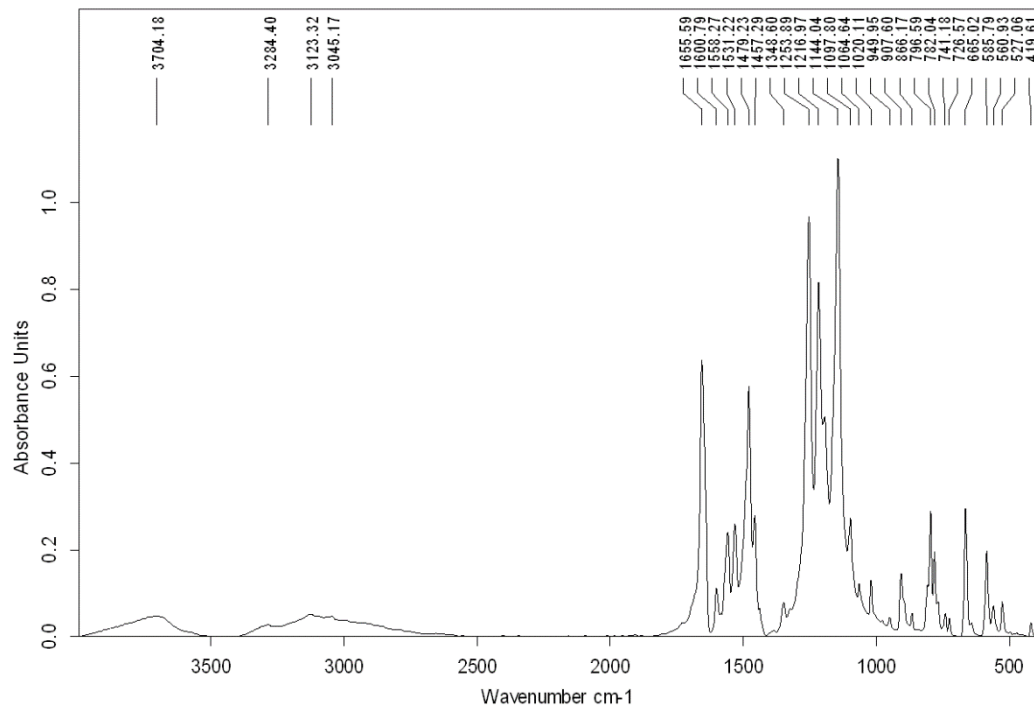


Figure S2. IR spectrum of compound 2.

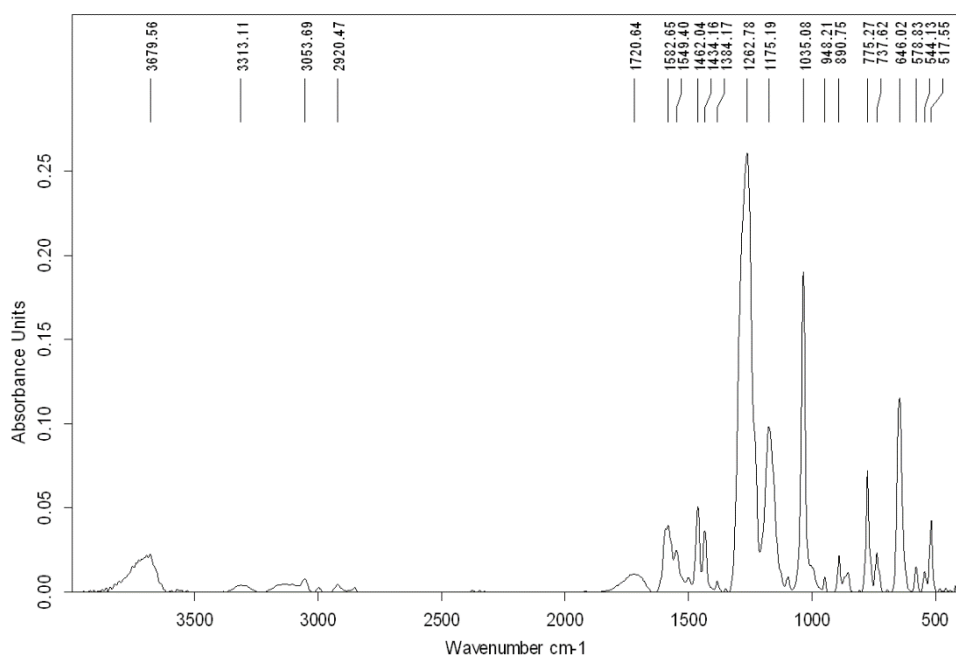


Figure S3. IR spectrum of compound 3.

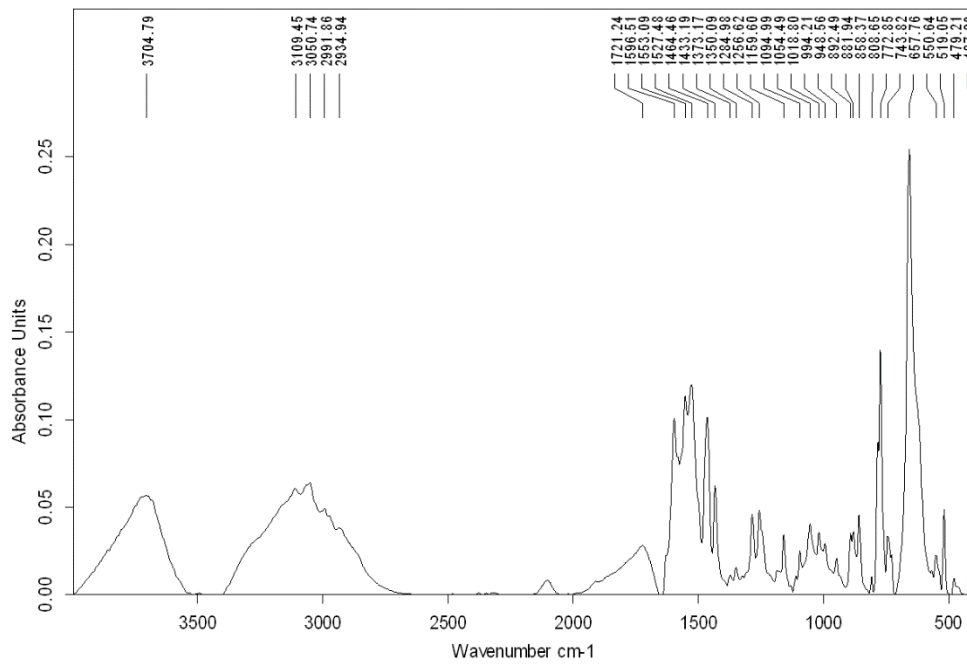


Figure S4. IR spectrum of compound 4.

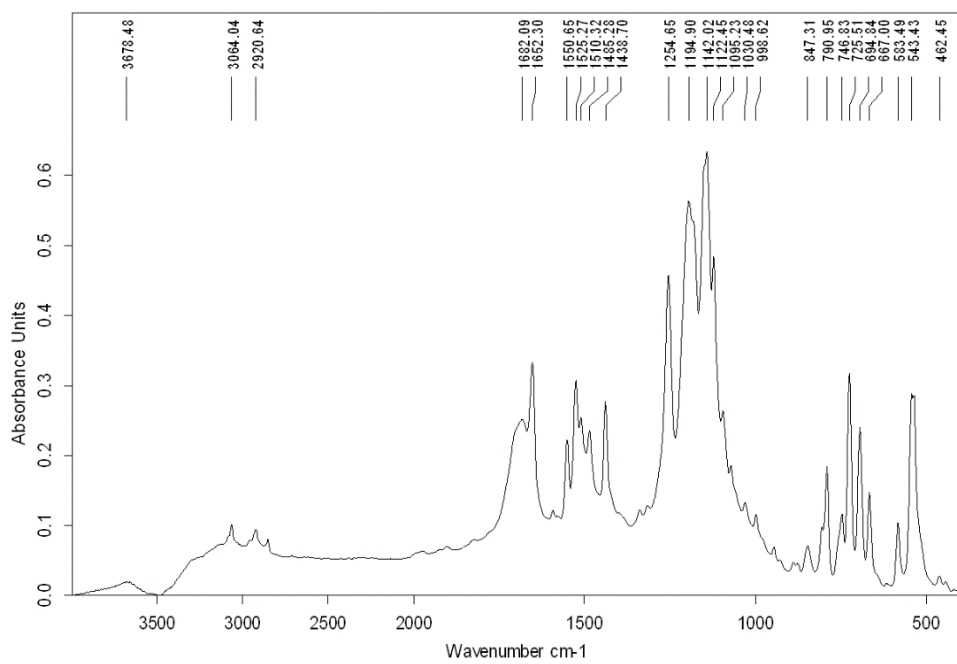


Figure S5. IR Spectrum of compound 6.

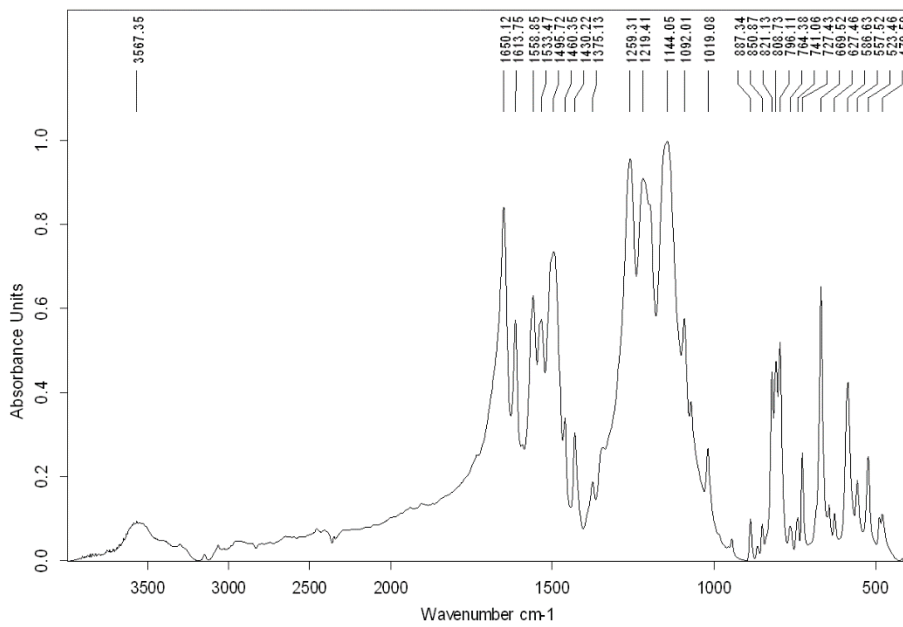


Figure S6. IR spectrum of compound 7.

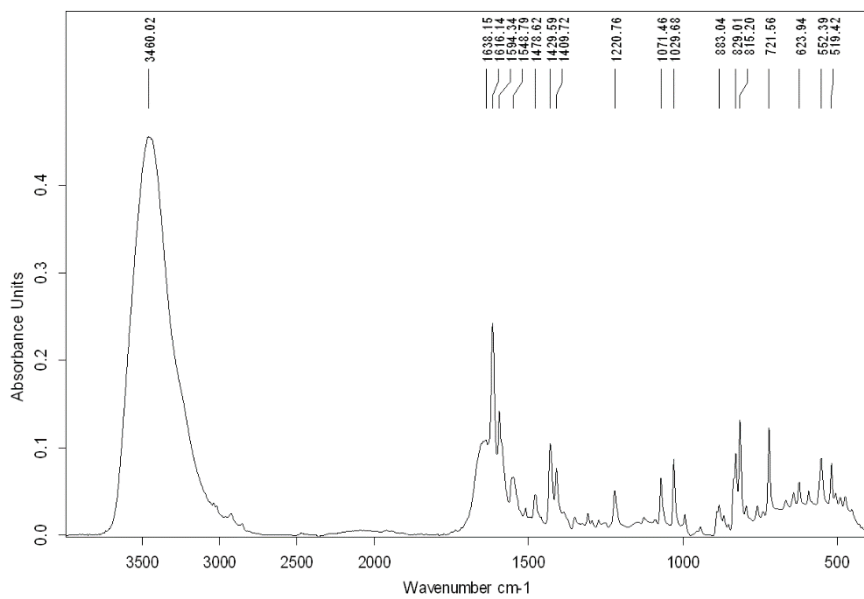


Figure S7. IR spectrum of compound 8.

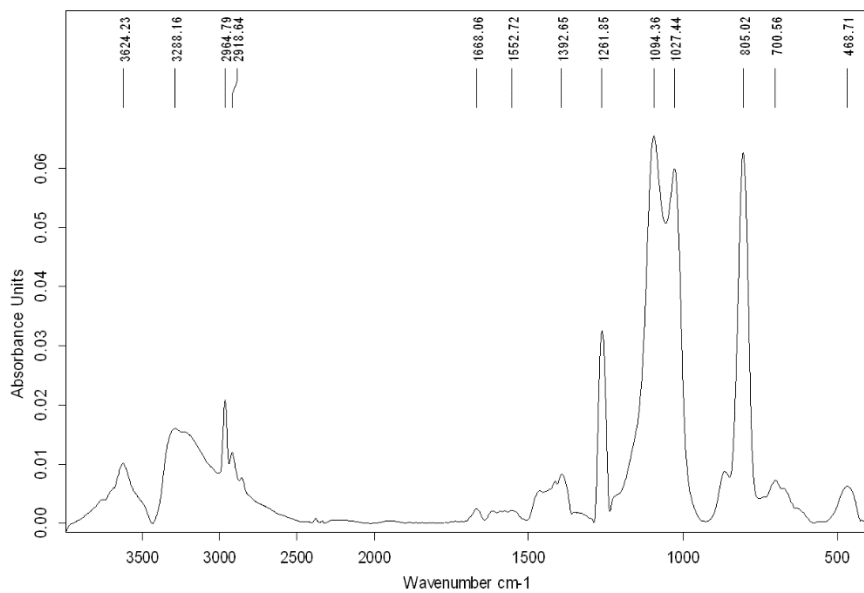


Figure S8. IR spectrum of compound 9.

Single crystal X-ray structures

Table S1. Crystallographic data, details of data collection and structure refinement parameters for compounds **1–5**.

	1	2	3	4	5
Formula sum	C ₂₆ H ₁₂ ZnF ₁₂ N ₄ O ₄ S	C ₃₆ H ₁₄ Zn ₂ F ₂₄ N ₄ O ₈ S	C ₁₇ H ₁₀ AgF ₃ N ₄ O ₃ S ₂	C ₁₆ H ₁₀ AgF ₆ SN ₄ Sb	C ₁₈ H ₁₃ Ag ₂ N ₇ O ₆ S
Formula weight	769.83	1249.32	547.28	633.96	671.15
Crystal system	monoclinic	monoclinic	monoclinic	monoclinic	monoclinic
Space group	P2 ₁ /c	C2/c	P2 ₁ /c	P2 ₁ /c	P2 ₁ /c
<i>a</i> /Å	8.7180(3)	21.6672(9)	8.2428(2)	8.0127(3)	13.1769(7)
<i>b</i> /Å	18.8045(6)	11.8405(5)	17.0241(3)	17.8981(5)	8.1432(4)
<i>c</i> /Å	18.7479(7)	17.6833(7)	13.5645(3)	13.1292(4)	20.1443(13)
<i>α</i> /°	90	90	90	90	90
<i>β</i> /°	97.318(3)	104.248(4)	99.838(2)	100.024(3)	109.027(7)
<i>γ</i> /°	90	90	90	90	90
<i>V</i> /Å ³	3048.46(19)	4397.1(3)	1875.46(7)	1854.14(10)	2043.4(2)
<i>Z</i>	4	8	4	4	4
<i>D_c</i> /g cm ⁻³	1.677	1.887	1.938	2.271	2.182
T/K	293(2)	299.30(10)	150.01(10)	150.01(10)	150.00(10)
μ /mm ⁻¹	0.987	3.263	11.255	21.745	16.841
Reflections collected	23001	8511	7468	8044	5232
Independent reflection	7670 [<i>R</i> _{int} = 0.0471]	4242 [<i>R</i> _{int} = 0.0321]	3602 [<i>R</i> _{int} = 0.0318]	3542 [<i>R</i> _{int} = 0.0355]	3025 [<i>R</i> _{int} = 0.0338]
final <i>R</i> ₁ ^a , <i>wR</i> ₂ ^b [<i>I</i> > 2σ(<i>I</i>)]	0.0493 / 0.1218	0.0563 / 0.1619	0.0294 / 0.0764	0.0368 / 0.0880	0.0413 / 0.1096
<i>R</i> ₁ ^a , <i>wR</i> ₂ ^b (all data)	0.0946 / 0.1372	0.0611 / 0.1761	0.0336 / 0.0802	0.0430 / 0.0951	0.0448 / 0.1188
goodness-of-fit on F ²	1.017	1.080	1.029	1.045	1.072
$\Delta\rho_{\min}/\Delta\rho_{\max}$ (e Å ⁻³)	-0.33 / 0.47	-0.70 / 1.04	-0.52 / 0.75	-1.16 / 1.42	-1.61 / 0.93
Completeness (%)	100	99.7	99.9	99.3	78.4

^a*R*₁ = $\sum |F_o| - |F_c| | / \sum |F_o|$. ^b*wR*₂ = $[\sum w(F_o^2 - F_c^2)^2 / \sum w(F_o^2)^2]^{1/2}$; $w = 1 / [\sigma^2(F_o^2) + (aP)^2 + bP]$ where $P = [max(F_o^2, 0) + 2F_c^2]/3$.

Table S2. Crystallographic data, details of data collection and structure refinement parameters for compounds 6–9.

	6	7	8	9
Formula sum	C ₂₆ H ₁₂ ZnF ₁₂ N ₄ O ₄ S	C ₂₆ H ₁₂ ZnF ₁₂ N ₄ O ₄ S	C ₃₂ H ₂₀ ZnCl ₂ N ₈ S ₂	C ₁₆ H ₁₀ ZnCl ₂ N ₄ S
Formula weight	769.83	769.83	716.95	426.61
Crystal system	monoclinic	triclinic	monoclinic	orthorhombic
Space group	P2 ₁ /n	P-1	P2 ₁ /c	P2 ₁ 2 ₁ 2 ₁
a/Å	11.0639(4)	7.8997(2)	15.8461(5)	5.3930(3)
b/Å	11.9939(6)	10.5946(3)	13.2351(3)	13.7128(6)
c/Å	22.0792(9)	18.5587(5)	14.7753(4)	23.0313(10)
α/°	90	102.626(2)	90	90
β/°	97.577(4)	91.823(2)	103.854(3)	90
γ/°	90	97.573(2)	90	90
V/Å ³	2904.3(2)	1499.52(7)	3008.60(15)	1703.24(14)
Z	4	2	4	4
D _c /g cm ⁻³	1.761	1.705	1.583	1.664
T/K	299.00(10)	293(2)	293(2)	284(20)
μ/mm ⁻¹	2.96	1.004	1.172	6.077
Reflections collected	9145	19338	23855	4388
Independent reflection	9145[R _{int} = 0.0439]	7482[R _{int} = 0.0345]	7607[R _{int} = 0.0281]	2953[R _{int} = 0.0453]
final R ₁ ^a / wR ₂ ^b [I > 2σ(I)]	0.0451/0.1002	0.0487/0.1388	0.0335/ 0.0831	0.0578/ 0.1472
R ₁ ^a /wR ₂ ^b (all data)	0.0911/0.1163	0.0742/ 0.1557	0.0497/ 0.0887	0.0646/ 0.1630
goodness-of-fit on F ²	0.840	0.971	1.050	1.064
Δρ _{min} /Δρ _{max} (e Å ⁻³)	-0.46/0.94	-0.44/0.86	-0.32/0.45	-0.85/1.06
Completeness (%)	98.3	100	100	99.1
Flack parameter				-0.02(4)

^aR₁ = $\sum ||F_o| - |F_c|| / \sum |F_o|$. ^bwR₂ = $[\sum w(F_o^2 - F_c^2)^2 / \sum w(F_o^2)^2]^{1/2}$; w = $1 / [\sigma^2(F_o^2) + (aP)^2 + bP]$ where P = $[max(F_o^2, 0) + 2F_c^2]/3$.

Compounds [Zn(hfac)₂(2-PyBTD)] **1** and [Zn₂(hfac)₄(2-PyBTD)] **2**

Table S3. Selected bond angles (°) for compounds **1** and **2**.

	1		2
N1 Zn1 N2	88.0(3)	N1 Zn1 N2	86.8(1)
N1 Zn1 O1	169.6(3)	N1 Zn1 O1	165.6(1)
N1 Zn1 O2	86.9(2)	N1 Zn1 O2	89.9(1)
N1 Zn1 O3	103.9(2)	N1 Zn1 O3	104.4(2)
N1 Zn1 O4	95.7(3)	N1 Zn1 O4	97.8(1)
N2 Zn1 O1	88.5(2)	N2 Zn1 O1	83.0(1)
N2 Zn1 O2	103.5(3)	N2 Zn1 O2	104.6(1)
N2 Zn1 O3	84.1(2)	N2 Zn1 O3	82.7(1)
N2 Zn1 O4	167.3(3)	N2 Zn1 O4	168.1(2)
O1 Zn1 O2	84.5(2)	O1 Zn1 O2	82.7(1)
O1 Zn1 O3	85.4(2)	O1 Zn1 O3	84.4(1)
O1 Zn1 O4	89.9(2)	O1 Zn1 O4	94.0(1)
O2 Zn1 O3	167.1(2)	O2 Zn1 O3	164.2(2)
O2 Zn1 O4	88.9(3)	O2 Zn1 O4	86.3(1)
O3 Zn1 O4	83.2(3)	O3 Zn1 O4	85.5(2)

Compounds $[\text{Ag}(\text{CF}_3\text{SO}_3)(2\text{-PyBTD})]_2$ **3** and $[\text{Ag}(2\text{-PyBTD})]_2(\text{SbF}_6)_2$ **4**

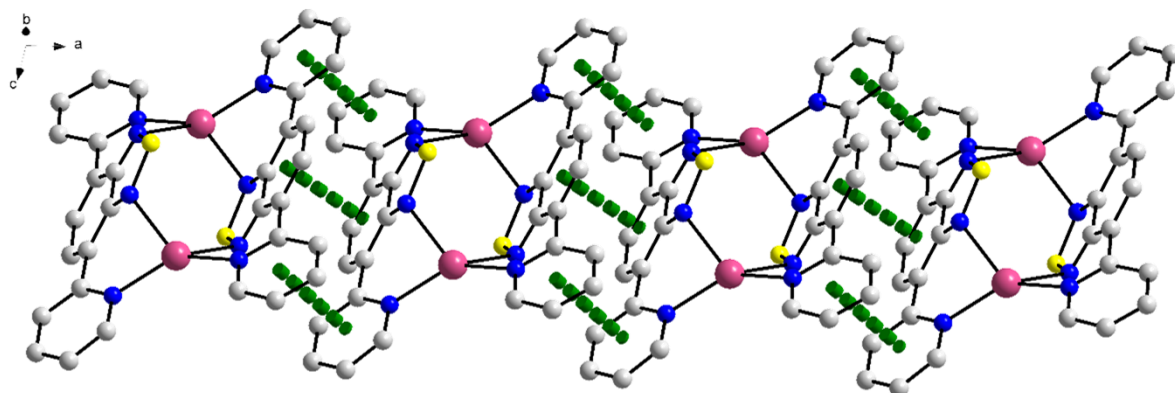


Figure S9. Perspective of the 1D supramolecular assembly in **4**.

Table S4. Selected bond angles ($^\circ$) for compounds **3** and **4**.

	3	4	
N1 Ag1 N2	81.5(1)	N1 Ag1 N2	79.2(2)
N1 Ag1 N3 ^a	114.6(1)	N1 Ag1 N3 ^a	136.3(2)
N1 Ag1 N4 ^a	135.9(1)	N1 Ag1 N4 ^a	140.9(2)
N2 Ag1 N3 ^a	94.2(9)	N2 Ag1 N3 ^a	91.8(2)
N2 Ag1 N4 ^a	142.5(1)	N2 Ag1 N4 ^a	119.2(2)
N3 ^a Ag1 N4 ^a	72.6(1)	N3 ^a Ag1 N4 ^a	80.3(2)
O1 Ag1 N1	97.7(9)		
O1 Ag1 N2	93.5(9)		
O1 Ag1 N3 ^a	147.4(8)		
O1 Ag1 N4 ^a	82.1(1)		

^a= $1-x, 1-y, 1-z$ ^a= $1-x, -y, 1-z$

Compound $[\text{Ag}_2(\text{NO}_3)_2(2\text{-PyBTD})(\text{CH}_3\text{CN})]$ 5

Table S5. Values of the SHAPE parameter for the Ag1 ion in compound 5 for hexacoordination.

	hexagon (D_{6h})	pentagonal pyramid (C_{5v})	octahedron (O_h)	trigonal prism (D_{3h})	Pentagonal pyramid Johnson (C_{5v})
5	25.457	8.704	25.129	12.497	13.012

Table S6. Selected bond angles ($^\circ$) for compound 5.

5			
N1 Ag1 O1	103.0(2)	O4 Ag1 O6 ^a	75.6(2)
N1 Ag1 O3	92.4(3)	O5 ^a Ag1 O6 ^a	48.3(2)
N1 Ag1 O4	126.5(2)	N2 A21 N4 ^b	115.7(2)
N1 Ag1 O5 ^a	101.8(2)	N2 Ag2 N7	133.0(2)
N1 Ag1 O6 ^a	134.9(2)	N2 Ag2 O6	74.9(2)
O1 Ag1 O3	47.3(2)	N2 Ag2 O5 ^c	125.8(2)
O1 Ag1 O4	102.4(2)	N4 ^b Ag2 O6	155.2(2)
O1 Ag1 O5 ^a	91.6(2)	N4 ^b Ag2 N7	99.3(2)
O1 Ag1 O6 ^a	109.6(2)	N4 ^b Ag2 O5 ^c	72.7(2)
O3 Ag1 O4	72.4(2)	N7 Ag2 O6	86.1(2)
O3 Ag1 O5 ^a	138.8(2)	N7 Ag2 O5 ^c	92.8(2)
O3 Ag1 O6 ^a	132.4(2)	O6 Ag2 O5 ^c	82.9(2)
O4 Ag1 O5 ^a	123.4(2)		

^a=1-x, 0.5+y, 0.5-z; ^b=1-x, 1-y, 1-z; ^c=1-x, -0.5+y, 0.5-z

Compound $[\text{Zn}(\text{hfac})_2(3\text{-PyBTD})]$ (**6**).

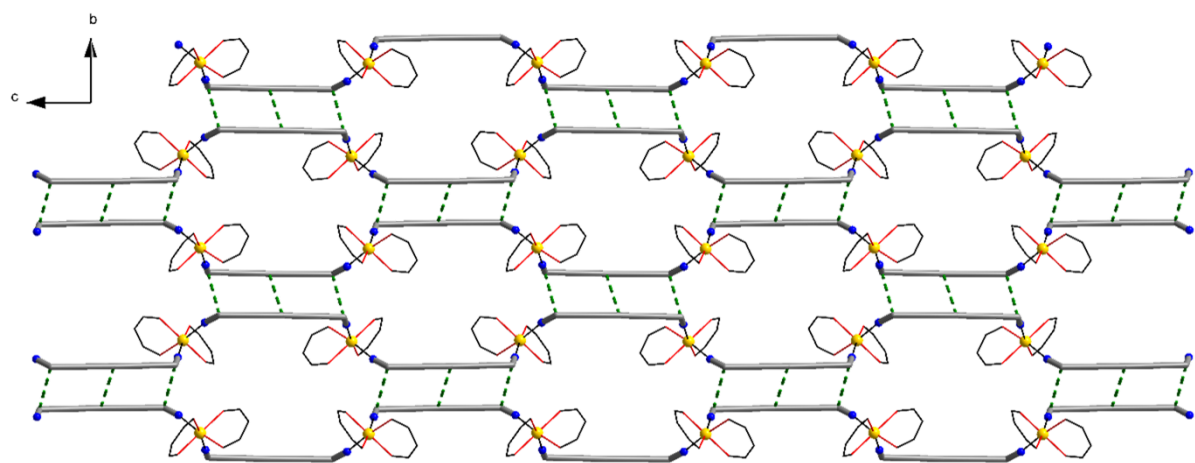


Figure S10. Schematic representation of the supramolecular layer in crystal structure of **6**.

Table S7. Selected bond angles ($^{\circ}$) for compound **6**.

6			
O1 Zn1 O2	84.9(1)	O2 Zn1 N4 ^a	94.7(2)
O1 Zn1 O3	93.3(2)	O3 Zn1 O4	84.7(2)
O1 Zn1 O4	177.1(2)	O3 Zn1 N1	96.0(2)
O1 Zn1 N1	89.3(2)	O3 Zn1 N4 ^a	173.8(2)
O1 Zn1 N4 ^a	91.8(2)	O4 Zn1 N1	92.9(2)
O2 Zn1 O3	82.4(1)	O4 Zn1 N4 ^a	89.9(2)
O2 Zn1 O4	94.7(2)	N1 Zn1 N4 ^a	87.3(2)
O2 Zn1 N1	173.9(2)		

^a= $x, -1.5 - y, -0.5 + z$

Compound [Zn(hfac)₂(4-PyBTD)] **7**

Table S8. Selected bond angles (°) for compound **7**.

7			
O1 Zn1 O2	89.0(1)	O3 Zn2 O4	89.4(1)
O1 Zn1 O1 ^a	180	O3 Zn2 O3 ^b	180
O1 Zn1 O2 ^a	91.0(1)	O3 Zn2 O4 ^b	89.1(2)
O1 Zn1 N1	90.1(2)	O3 Zn2 N4	90.8(2)
O1 Zn1 N1 ^a	89.8(2)	O3 Zn2 N4 ^b	89.1(2)
O2 Zn1 O1 ^a	91.0(1)	O4 Zn2 O3 ^b	90.6(1)
O2 Zn1 O2 ^a	180	O4 Zn2 O4 ^b	180
O2 Zn1 N1	88.0(2)	O4 Zn2 N4	90.2(2)
O2 Zn1 N1 ^a	91.9(1)	O4 Zn2 N4 ^b	89.7(1)
O1 ^a Zn1 O2 ^a	89.0(1)	O3 ^b Zn2 O4 ^b	89.3(2)
O1 ^a Zn1 N1	89.8(1)	O3 ^b Zn2 N4	89.1(2)
O1 ^a Zn1 N1 ^a	90.1(2)	O3 ^b Zn2 N4 ^b	90.8(1)
O2 ^a Zn1 N1	91.9(1)	O4 ^b Zn2 N4	89.7(1)
O2 ^a Zn1 N1 ^a	88.0(2)	O4 ^b Zn2 N4 ^b	90.2(2)
N1 Zn1 N1 ^a	180	N4 Zn2 N4 ^b	180

^a = -x, 2-y, 2-z; ^b = 2-x, -y, 1-z

Compound $[\text{ZnCl}_2(4\text{-PyBTD})_2]$ **8**

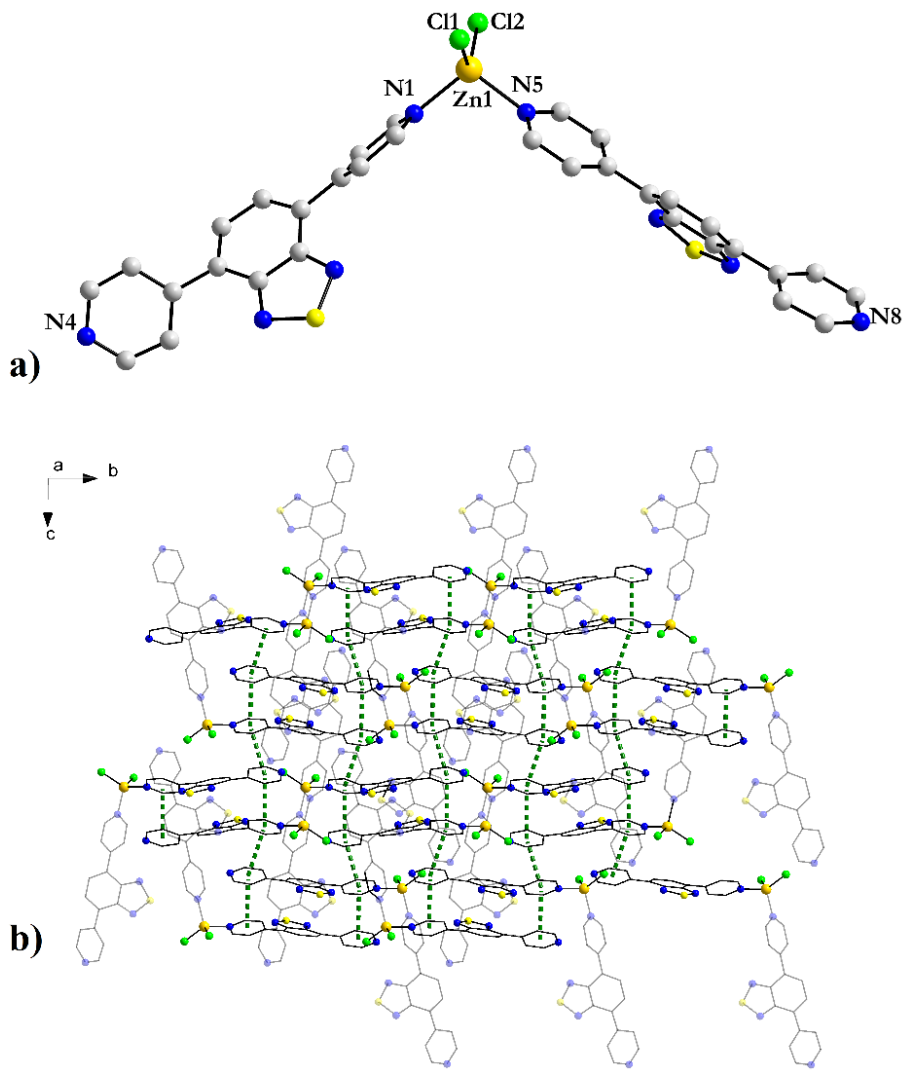


Figure S11. (a) Molecular structure of complex $[\text{ZnCl}_2(4\text{-PyBTD})_2]$ **8**; (b) Perspective view of the 2D layers resulting from $\pi-\pi$ stacking between pyridine rings from adjacent mononuclear species.

Table S9. Selected bond angles ($^\circ$) for compounds **8** and **9**.

	8	9	
N1 Zn1 N5	104.3(1)	N1 ^a Zn1 N4	106.1(3)
N1 Zn1 Cl1	105.5(1)	N1 ^a Zn1 Cl1	105.5(2)
N1 Zn1 Cl2	110.9(2)	N1 ^a Zn1 Cl2	104.3(2)
N5 Zn1 Cl1	105.9(2)	N4 Zn1 Cl1	106.9(2)
N5 Zn1 Cl2	108.5(1)	N4 Zn1 Cl2	105.0(2)
Cl1 Zn1 Cl2	120.3(1)	Cl1 Zn1 Cl2	127.3(2)

^a= $1.5-x, 1-y, 0.5+z$

X-Ray Powder Diffraction

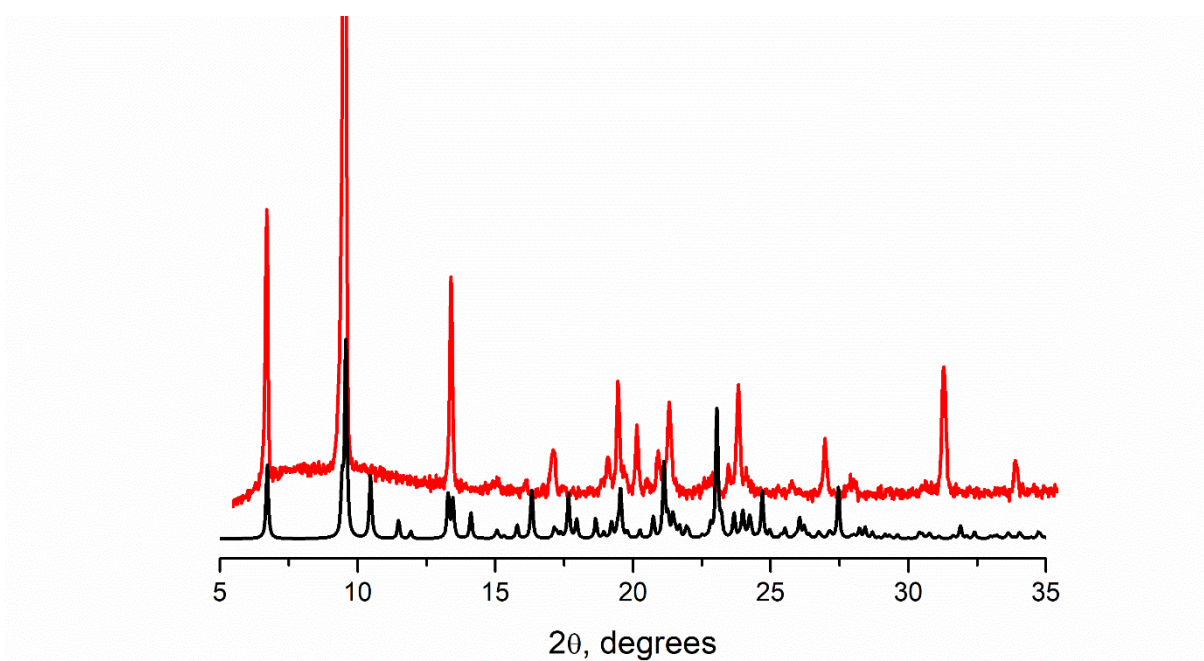


Figure S12. Simulated (black) and experimental (red) powder X-ray diffractograms for compound **1**. The peak observed at 32° arises from the sample holder.

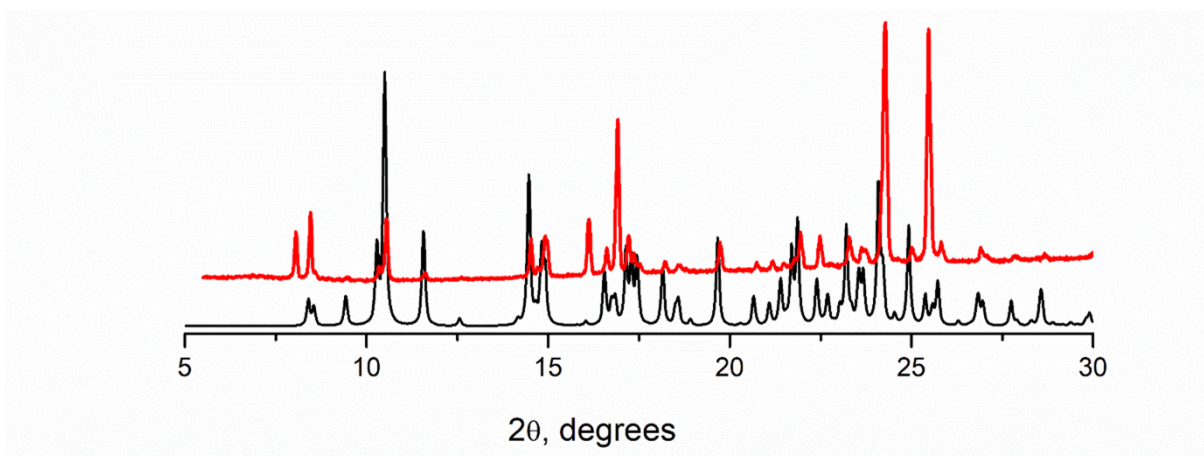


Figure S13. Simulated (black) and experimental (red) powder X-ray diffractograms for compound **2**.

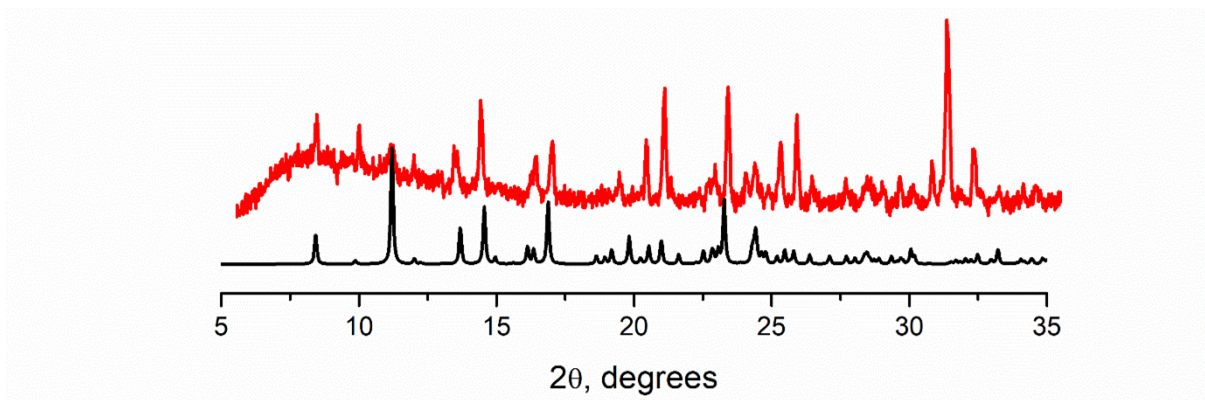


Figure S14. Simulated (black) and experimental (red) powder X-ray diffractograms for compound **4**. The peak observed at 32° arises from the sample holder.

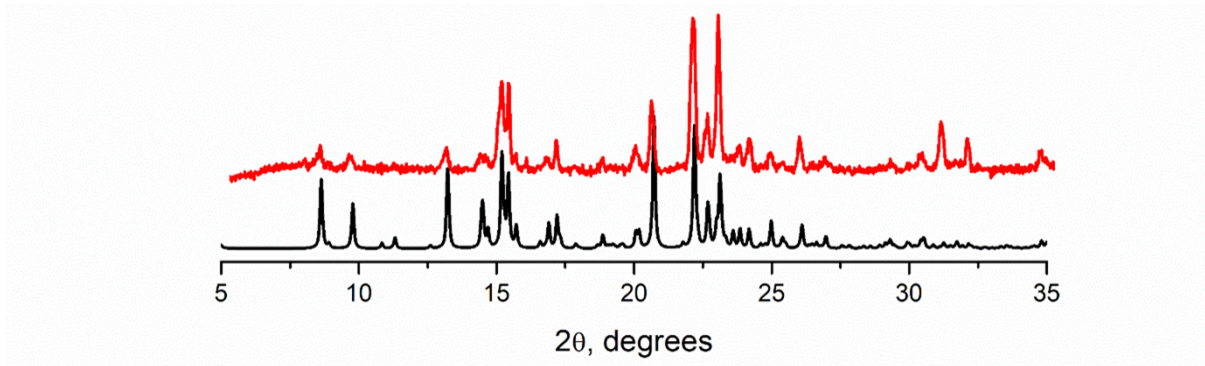


Figure S15. Simulated (black) and experimental (red) powder X-ray diffractograms for compound **7**.

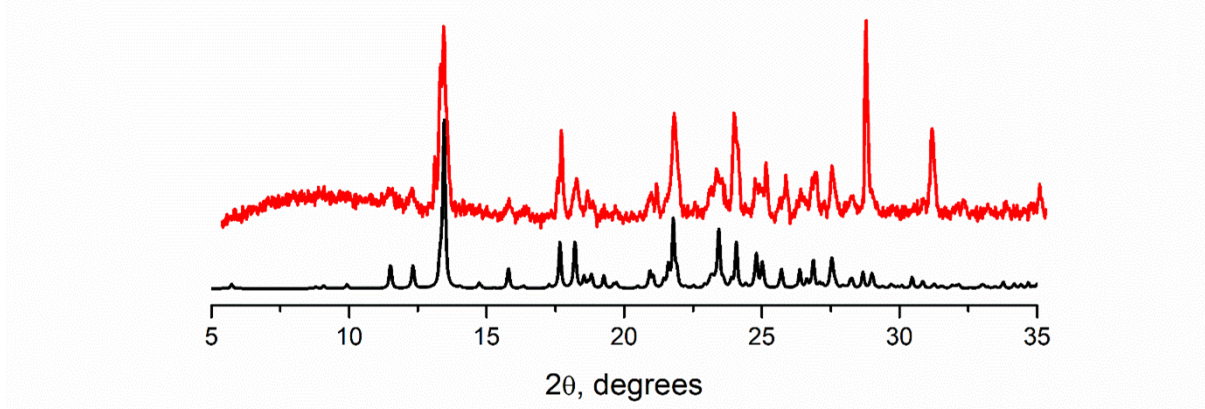


Figure S16. Simulated (black) and experimental (red) powder X-ray diffractograms for compound **8**. The peak observed at 32° arises from the sample holder.

Photophysical properties

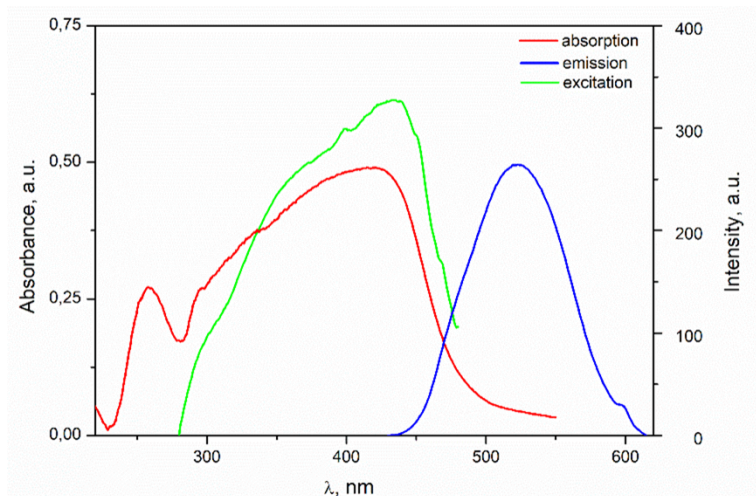


Figure S17. Solid state UV-Vis absorption spectrum (red curve), emission spectrum (blue curve, $\lambda_{\text{ex}} = 400$ nm) and excitation spectrum (green curve, $\lambda_{\text{em}} = 525$ nm) of ligand 2-PyBTD.

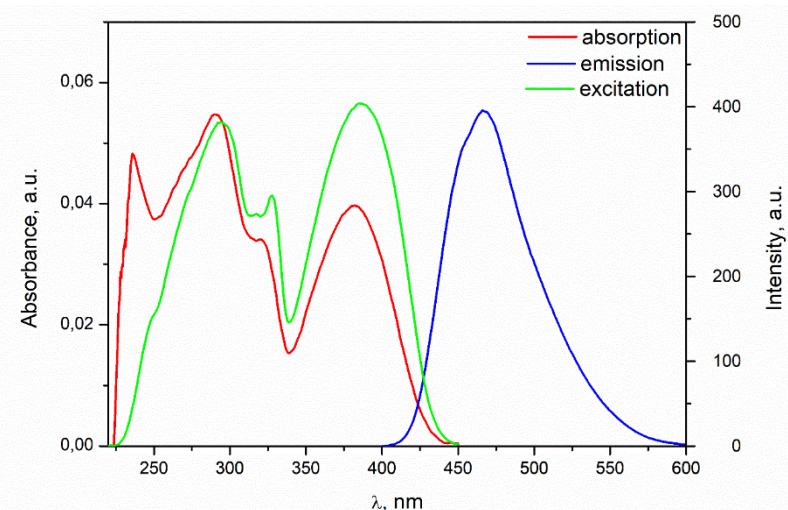


Figure S18. Absorption (red), emission (blue) and excitation (green) spectra of 2-PyBTD recorded in CH_2Cl_2 . (Absorption: $\lambda = 236, 290, 382$ nm; Emission: $\lambda_{\text{ex}} = 380$ nm, $\lambda_{\text{max}} = 466$ nm; Excitation: $\lambda_{\text{em}} = 465$ nm, $\lambda = 292, 385$ nm).

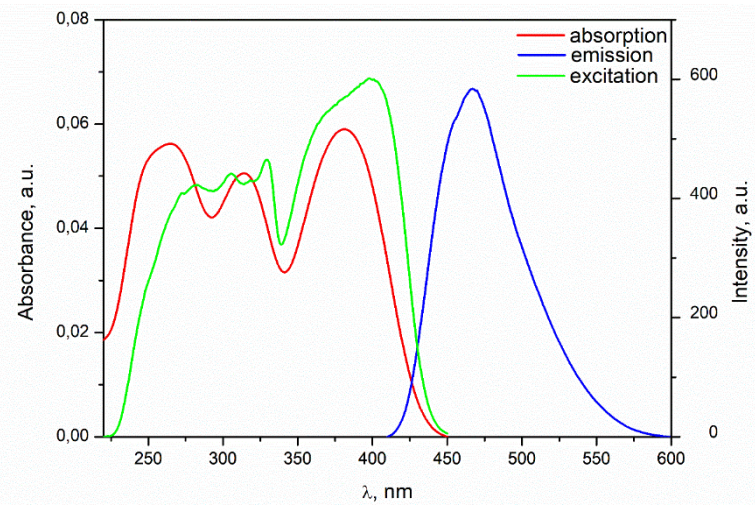


Figure S19. Absorption (red), emission (blue) and excitation (green) spectra of compound **1** recorded in CH_2Cl_2 . (Absorption: $\lambda = 265, 314, 381 \text{ nm}$; Emission: $\lambda_{\text{ex}} = 390 \text{ nm}$, $\lambda_{\text{max}} = 467 \text{ nm}$; Excitation: $\lambda_{\text{em}} = 465 \text{ nm}$, $\lambda = 282, 305, 329, 398 \text{ nm}$).

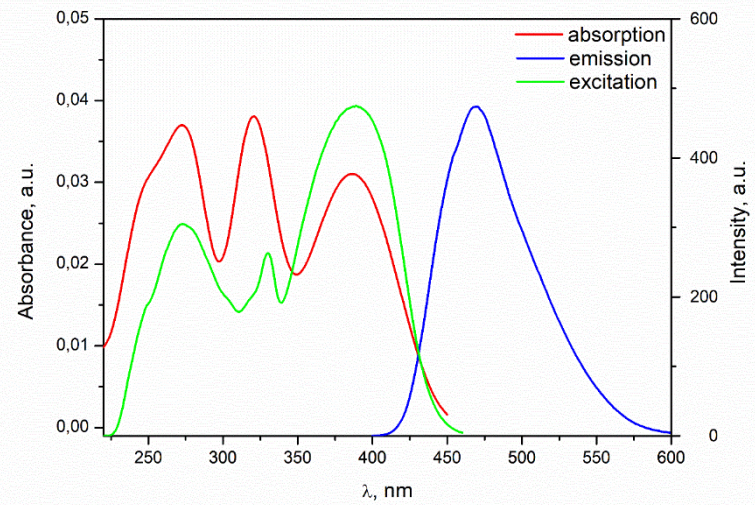


Figure S20. Absorption (red), emission (blue) and excitation (green) spectra of compound **2** recorded in CH_2Cl_2 . (Absorption: $\lambda = 272, 321, 387 \text{ nm}$; Emission: $\lambda_{\text{ex}} = 390 \text{ nm}$, $\lambda_{\text{max}} = 470 \text{ nm}$; Excitation: $\lambda_{\text{em}} = 470 \text{ nm}$, $\lambda = 273, 330, 389 \text{ nm}$).

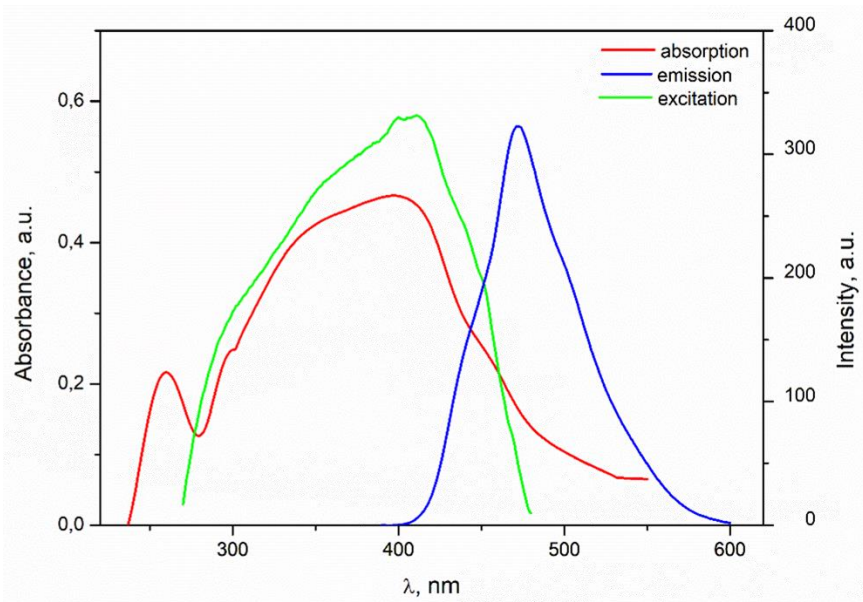


Figure S21. UV-Vis absorption spectrum (red curve), emission spectrum (blue curve, $\lambda_{\text{ex}} = 370$ nm) and excitation spectrum (green curve, $\lambda_{\text{em}} = 470$ nm) of ligand 4-PyBTD.

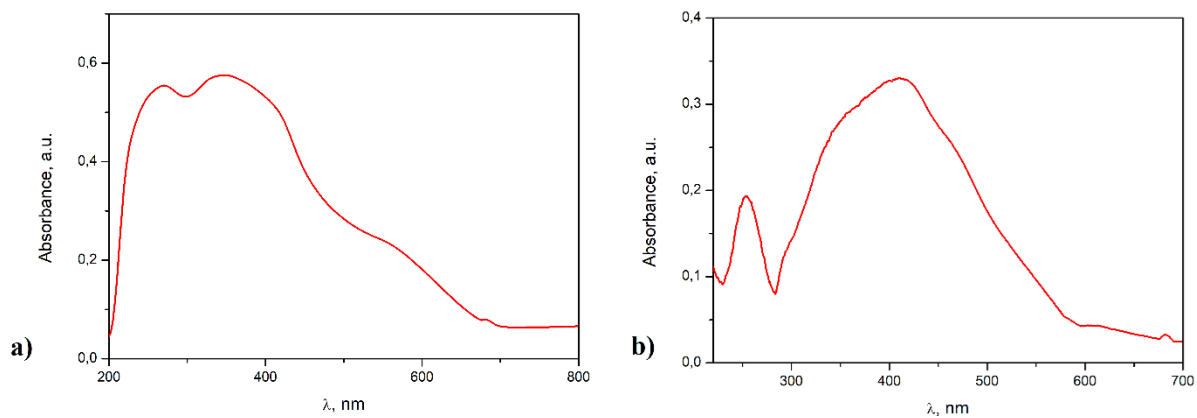


Figure S22. (a) UV-Vis absorption spectra of complex 8; (b) UV-Vis absorption spectra of complex 9.

DFT and TD-DFT calculations

Complex 1

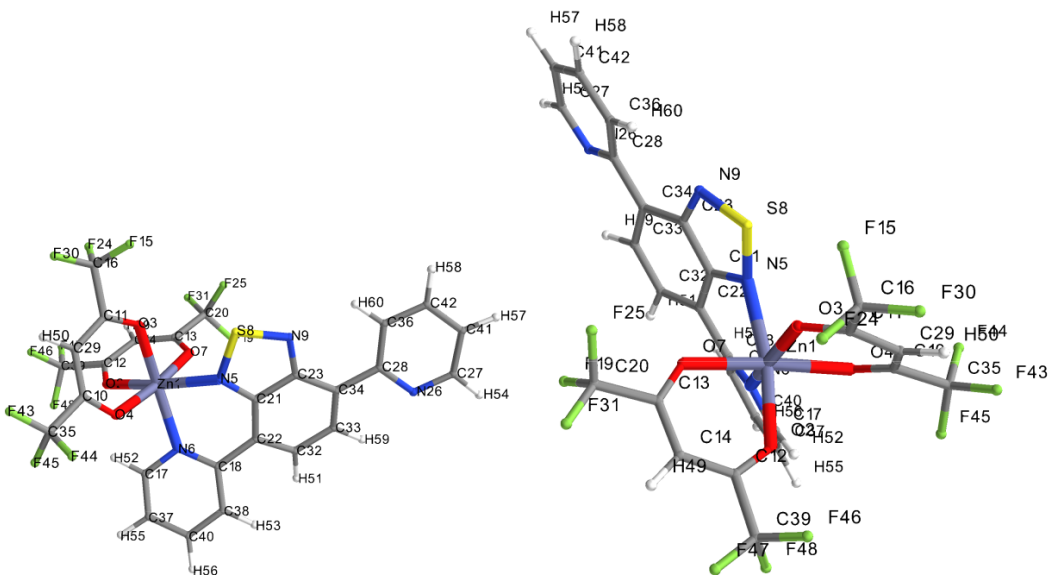


Figure S23. Two views of the optimized geometry of **1** together with the atom numbering scheme.

Total molecular energy	-4891.47820 hartrees
HOMO number	191
LUMO+1 energies	-2.19 eV
LUMO energies	-3.48 eV
HOMO energies	-7.11 eV
HOMO-1 energies	-7.28 eV
CDFT indices: Electron Affinity	0.0030 hartrees
CDFT indices: Ionisation Potential	0.0111 hartrees
CDFT indices: Electronegativity	0.0071 hartrees
CDFT indices: Hardness	0.0080 hartrees
CDFT indices: Electrophilicity	0.0031
CDFT indices: Electron-flow	0.8777 e-
Geometry optimization specific results	
Converged nuclear repulsion energy	8017.57621 Hartrees
Frequency and Thermochemistry specific results	
Number of negative frequencies	0
Sum of electronic and zero-point energy	-4891.11226 Hartrees
Sum of electronic and thermal energies at 298.15 K	-4891.06905 Hartrees
Enthalpy at 298.15 K	-4891.06811 Hartrees
Gibbs free energy at 298.15 K	-4891.20030 Hartrees
Entropy at 298.15 K	0.00044 Hartrees

Calculated mono-electronic excitations

E.S.	Symmetry	nm	cm-1	f	R	Lambda	dCT	qCT	Excitation description in %
1	Singlet-A	413	24205	0.307	19.245	0.72	234.22	0.52	191->192 (98)
2	Singlet-A	395	25283	0.008	3.855	0.13	505.10	0.96	190->192 (98)
3	Singlet-A	387	25812	0.002	3.093	0.14	499.06	0.96	189->192 (98)
4	Singlet-A	347	28817	0.003	5.782	0.28	221.10	0.87	186->192 (9) 187->192 (86)
5	Singlet-A	342	29165	0.002	1.083	0.13	457.59	0.96	188->192 (98)
6	Singlet-A	328	30484	0.004	-12.260	0.22	262.48	0.88	186->192 (85) 187->192 (9)
7	Singlet-A	315	31733	0.000	0.743	0.45	95.47	0.65	186->193 (8) 186->194 (6) 187->193 (2) 188->193 (41) 188->194 (30)
8	Singlet-A	311	32131	0.001	2.643	0.41	196.54	0.67	186->193 (19) 186->194 (19) 186->195 (4) 187->193 (5) 187->194 (5) 188->193 (15) 188->194 (17) 188->195 (4)
9	Singlet-A	300	33225	0.010	4.138	0.61	201.15	0.55	184->192 (24) 185->192 (71)
10	Singlet-A	293	34066	0.244	184.733	0.48	504.81	0.63	184->192 (3) 190->193 (2) 191->193 (6) 191->194 (21) 191->195 (60)

Atomic charges population analysis. Selection of the most charged atoms based on Hirshfeld analysis

Atom and N°	Hirshfeld charge	CM5 charge	Mulliken charge
N 6	-0.379	-0.134	-0.027
N 26	-0.375	-0.178	+0.009
N 9	-0.344	-0.173	-0.057
O 3	-0.337	-0.259	-0.376
O 2	-0.335	-0.248	-0.366
O 7	-0.332	-0.253	-0.334
O 4	-0.332	-0.250	-0.337
N 5	-0.251	-0.167	-0.119
C 16	+0.216	+0.234	+0.367
C 20	+0.217	+0.234	+0.356
S 8	+0.342	+0.349	+0.408
Zn 1	+0.711	+0.393	+0.912

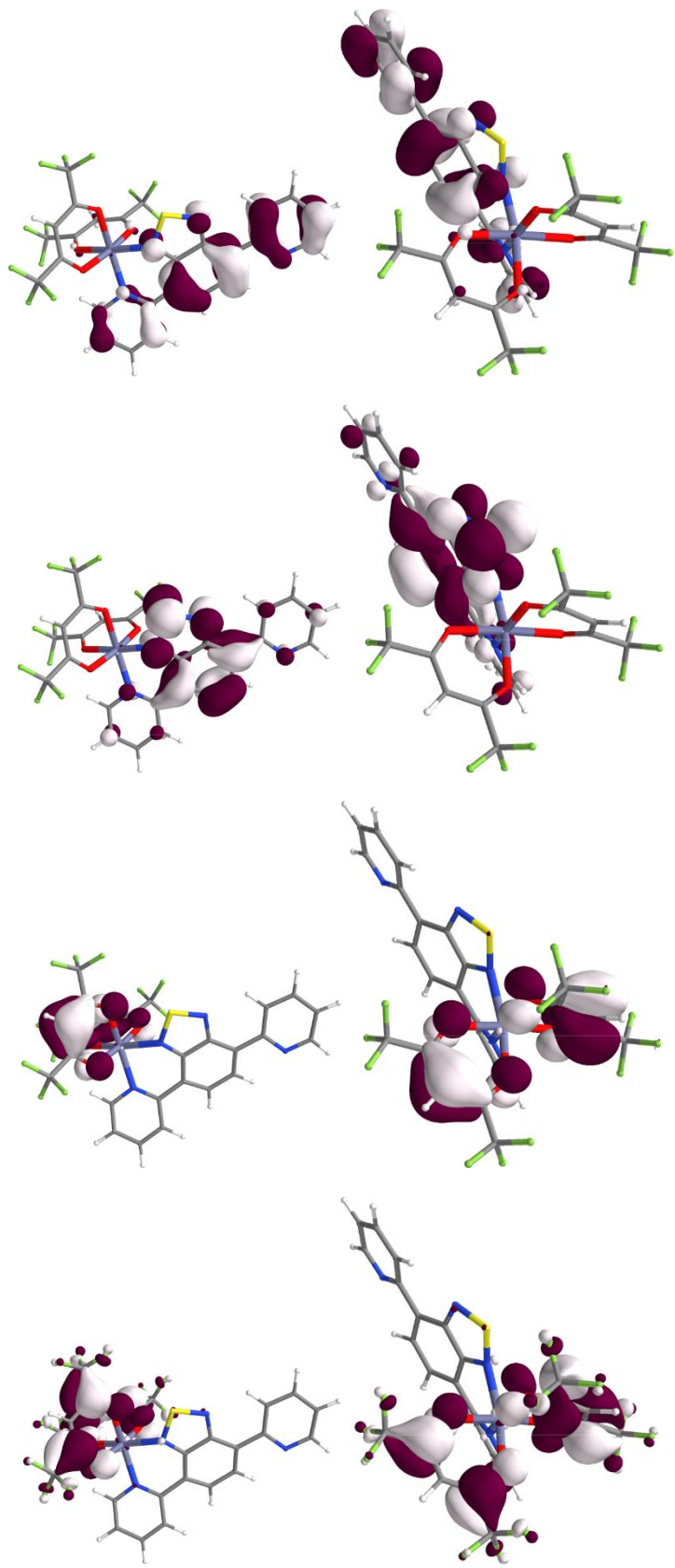


Figure S24. HOMO, LUMO, HOMO-1 and LUMO+1 (from top to bottom, two views each) of complex **1**.

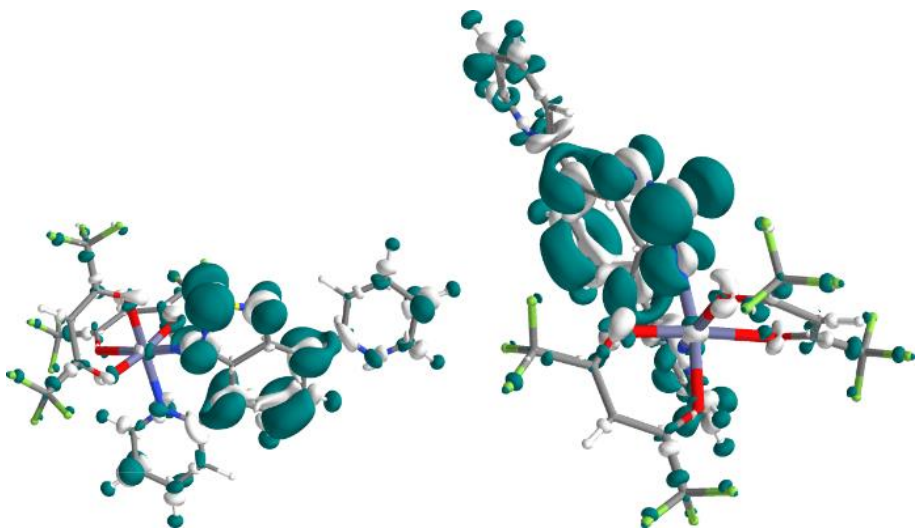


Figure S25. Representation of the F+ function (two views) for complex **1**. The blue color indicates the most electrophilic regions.

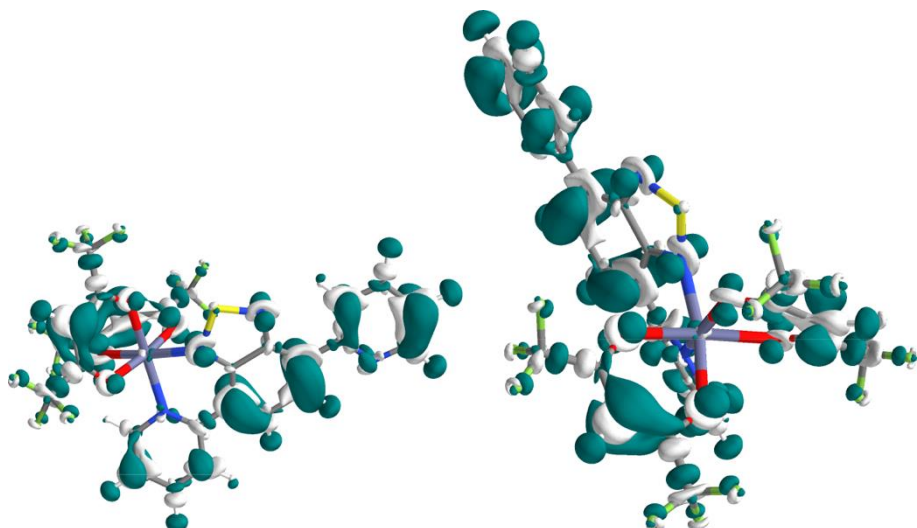


Figure S26. Representation of the F- function (two views) for complex **1**. The blue color indicates the most nucleophilic regions.

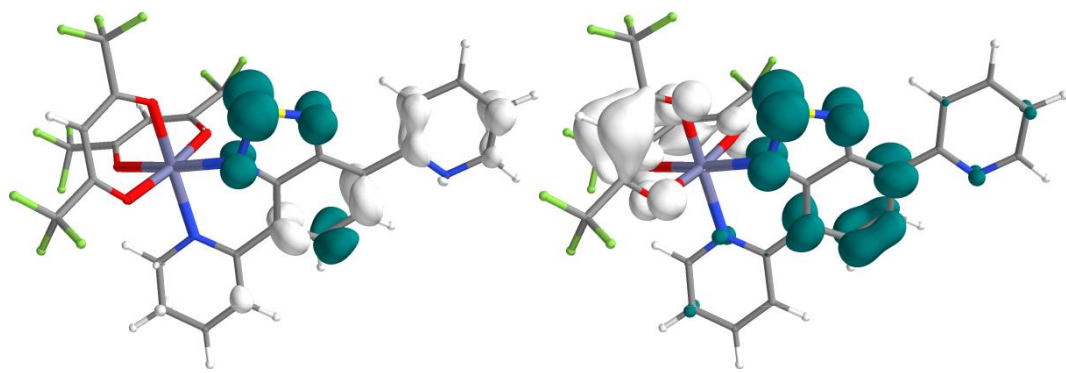


Figure S27. Representation of the Electron Density Difference (S1-S0 left) and (S2-S0 right) for complex 1. The excited electron and the hole regions are indicated by, respectively, blue and white surfaces.

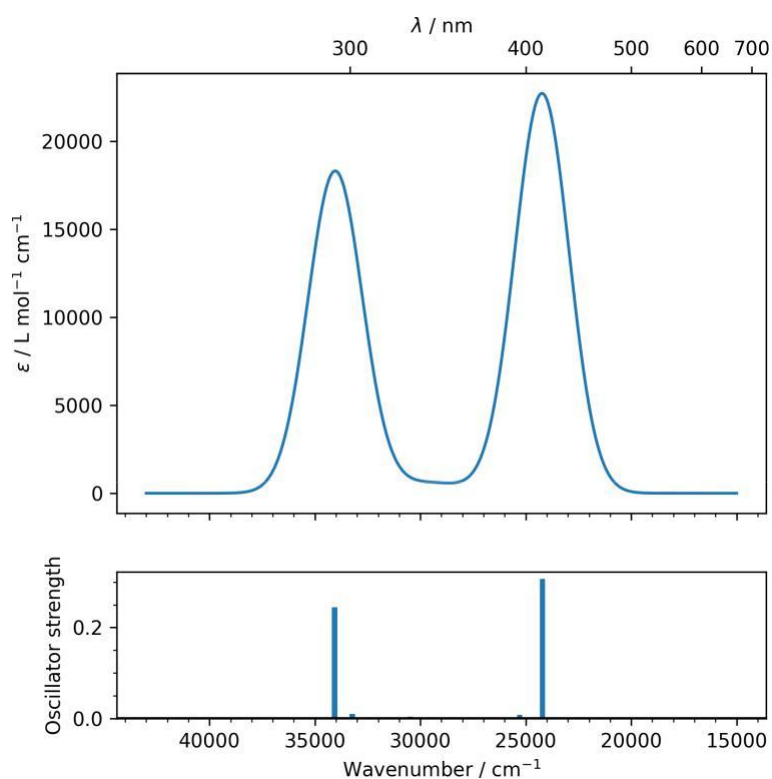


Figure S28. Calculated UV-visible absorption spectrum of complex 1 with a gaussian broadening (FWHM = 3000 cm⁻¹).

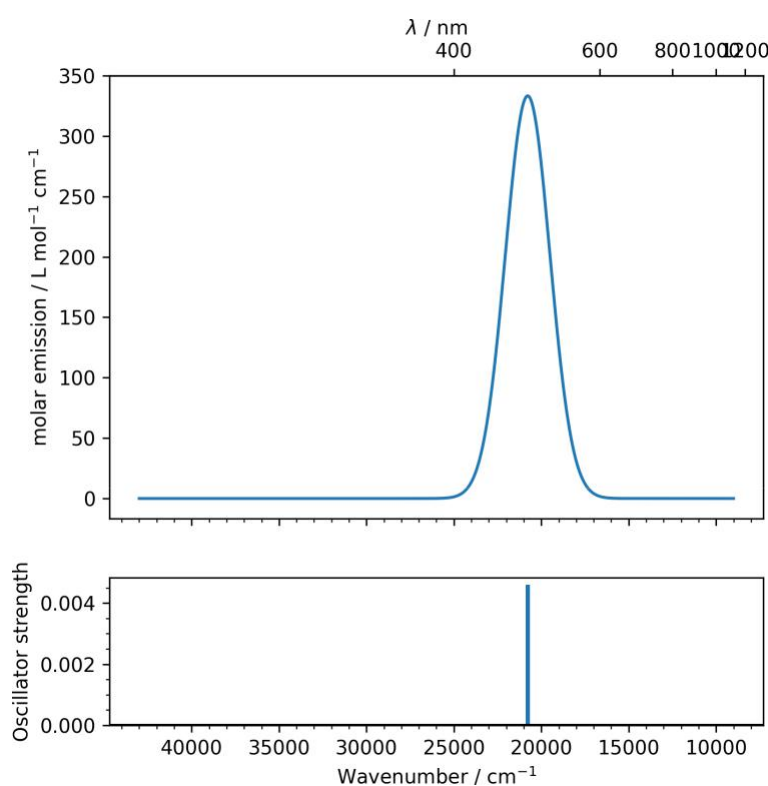


Figure S29. Calculated UV-visible emission spectrum of complex **1** with a gaussian broadening (FWHM = 3000 cm^{-1}).

Complex 2

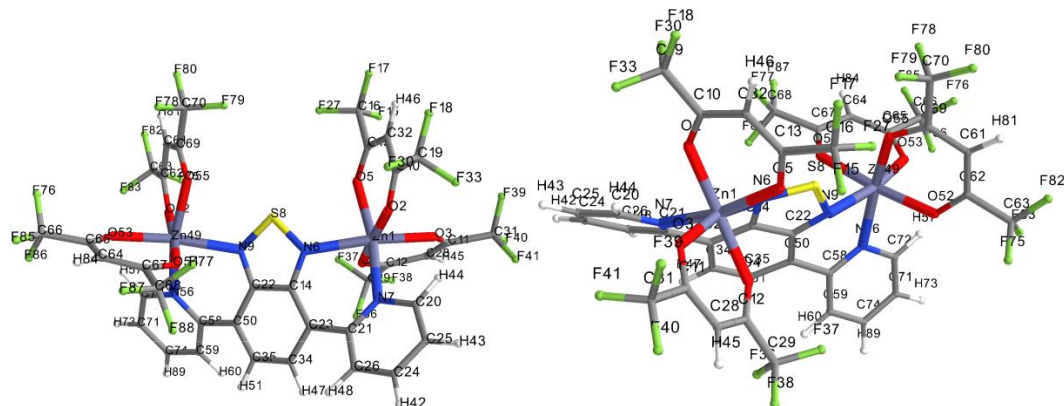


Figure S30. Two views of the optimized geometry of **2** together with the atom numbering scheme.

Total molecular energy	-8550.88880 hartrees
HOMO number	307
LUMO+1 energies	-2.61 eV
LUMO energies	-4.00 eV
HOMO energies	-7.48 eV
HOMO-1 energies	-7.49 eV

Geometry optimization specific results	
Converged nuclear repulsion energy	17624.10655 Hartrees
Frequency and Thermochemistry specific results	
Number of negative frequencies	0
Sum of electronic and zero-point energy	-8550.38636 Hartrees
Sum of electronic and thermal energies at 298.15 K	-8550.31530 Hartrees
Enthalpy at 298.15 K	-8550.31436 Hartrees
Gibbs free energy at 298.15 K	-8550.51627 Hartrees
Entropy at 298.15 K	0.00068 Hartrees

Calculated mono-electronic excitations

E.S.	Symmetry	nm	cm ⁻¹	f	R	Lambda	dCT	qCT	Excitation description in %
	Singlet-A	443	22534						
1	0.001				-1.690	0.15	369.30	0.97	307->308 (99)
	Singlet-A	442	22610						
2	0.006				-8.227	0.16	352.27	0.97	306->308 (99)
	Singlet-A	430	23231						
3	0.023				8.493	0.25	134.27	0.92	305->308 (99)
	Singlet-A	428	23319						
4	0.000				-1.429	0.11	160.90	0.98	304->308 (99)
	Singlet-A	397	25149						
5	0.265				-64.387	0.71	178.53	0.52	303->308 (98)
	Singlet-A	377	26471						
6	0.005				-0.930	0.17	277.70	0.95	302->308 (98)
	Singlet-A	377	26501						
7	0.001				-6.138	0.17	278.37	0.95	301->308 (98)
	Singlet-A	355	28168	0.003	8.127	0.19	183.65	0.92	300->308 (97)
8									
9	350		28537	0.006	16.209	0.20	175.38	0.93	299->308 (98)

Atomic charges population analysis. Selection of the most charged atoms based on Hirshfeld analysis

Atom and N°	Hirshfeld charge	CM5 charge	Mulliken charge
N 56	-0.377	-0.132	-0.024
N 7	-0.377	-0.132	-0.024
O 55	-0.340	-0.258	-0.378
O 5	-0.339	-0.258	-0.378
O 54	-0.335	-0.255	-0.345
O 4	-0.335	-0.255	-0.345
O 53	-0.334	-0.248	-0.358
O 3	-0.334	-0.248	-0.358
O 52	-0.334	-0.249	-0.342
O 2	-0.334	-0.249	-0.342
N 9	-0.263	-0.152	-0.098
N 6	-0.226	-0.152	-0.098
C 16	+0.217	+0.235	+0.371
C 19	+0.218	+0.236	+0.357
S 8	+0.400	+0.406	+0.507
Zn 49	+0.598	+0.396	+0.912
Zn 1	+0.712	+0.396	+0.912

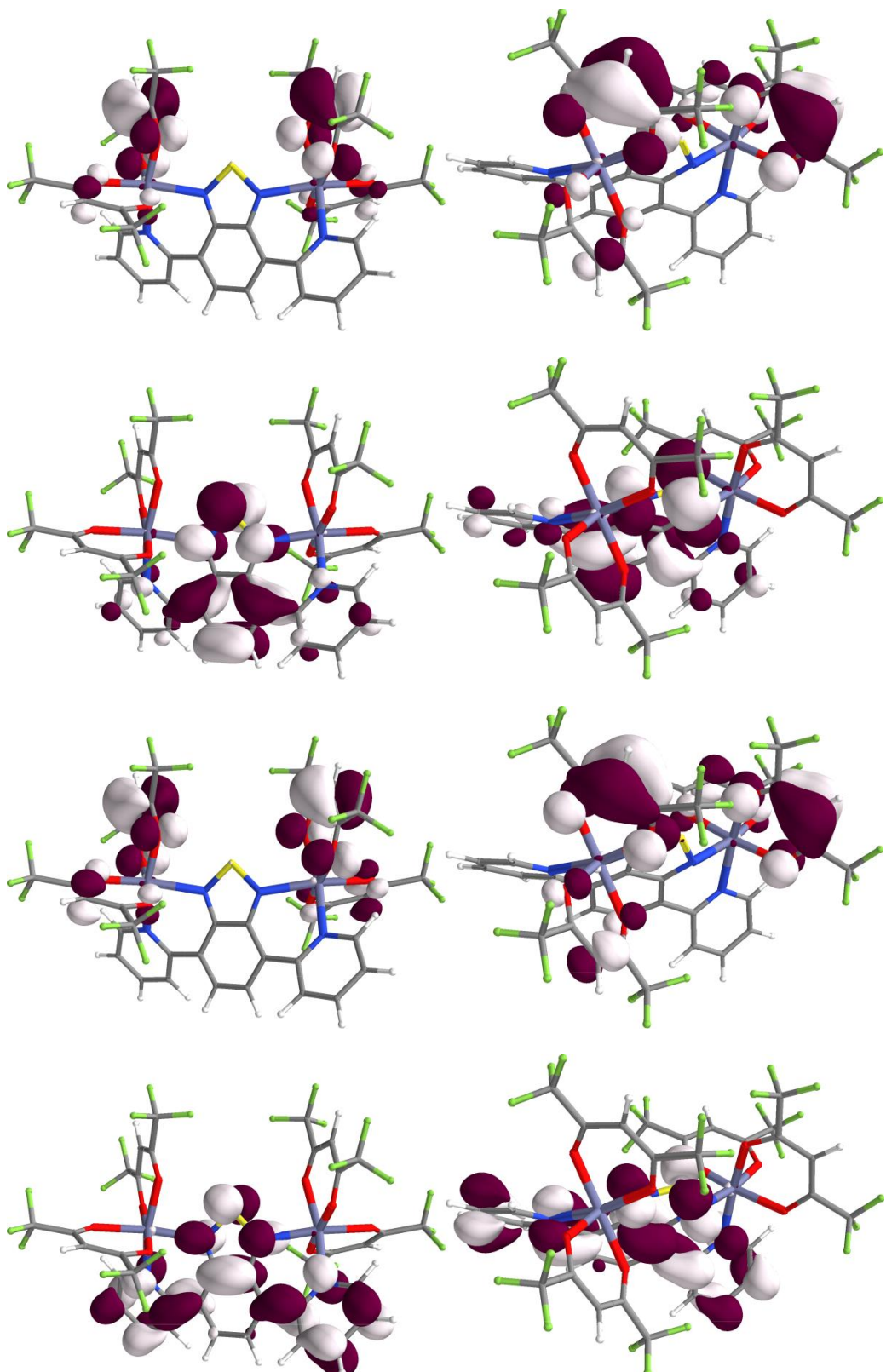


Figure S31. HOMO, LUMO, HOMO-1 and LUMO+1 (from top to bottom, two views each) of complex **2**.

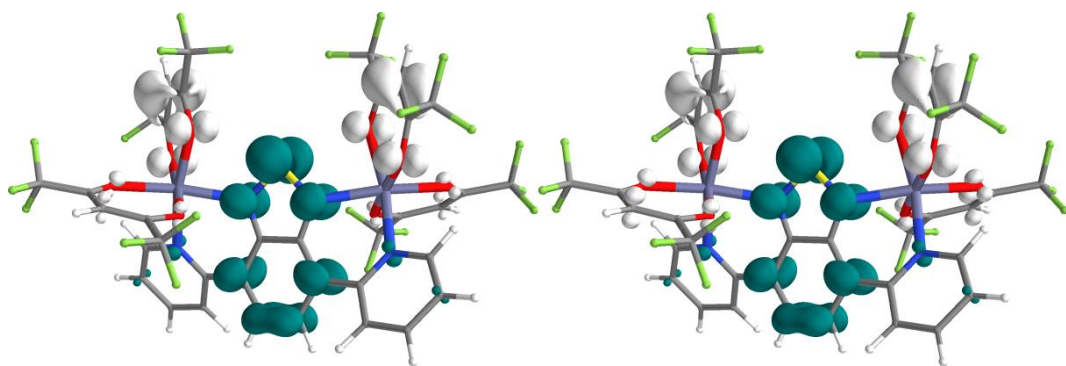


Figure S32. Representation of the Electron Density Difference (S1-S0 left) and (S2-S0 right) for complex **2**. The excited electron and the hole regions are indicated by, respectively, blue and white surfaces.

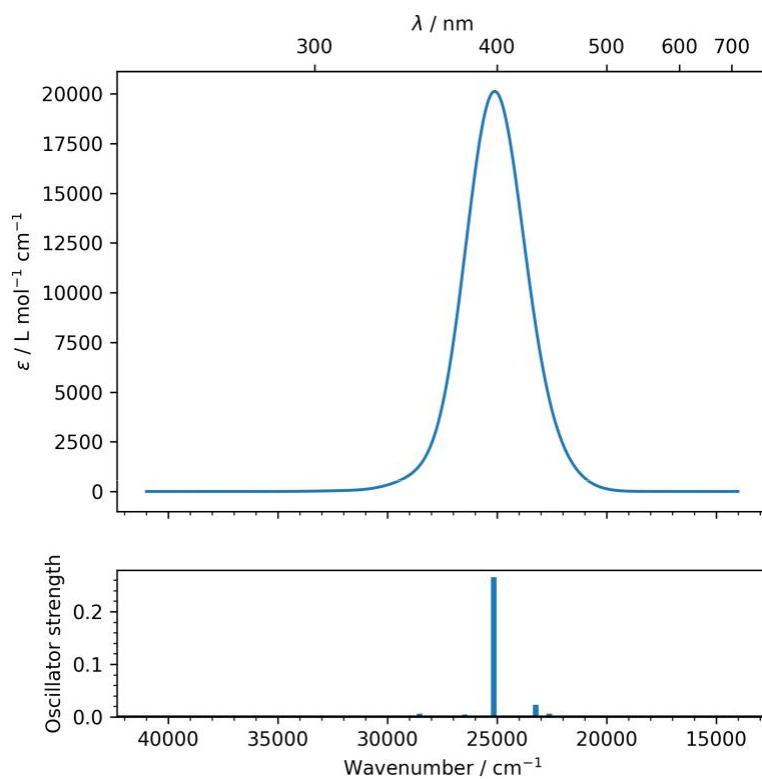


Figure S33. Calculated UV-visible absorption spectrum of complex **2** with a gaussian broadening (FWHM = 3000 cm^{-1}).